Journal of Environmental Science and Engineering A 14 (2025) 72-78
doi:10.17265/2162-5298/2025.01.007

Modeling of the Soil-Water Characteristic Curve—Case Study in Bom Brinquedo Hill's, Antonina, Brazil

Gislaine Klenk Malinoski and Vitor Pereira Faro
Federal University of Paraná, Curitiba 81530-000, Brazil

Abstract: In this paper, we present a modeling of the soil-water characteristic curve for residual and sedimentary soils of Bom Brinquedo Hill's, located in Antonina, Brazil. This mountain range region is characterized as a natural disaster risk area, requiring continuous research related to the stability of the area. To obtain the soil-water characteristic curve, undisturbed samples of residual and sedimentary soil were collected, followed by suction testing using the filter paper method. Considering the bimodal characteristic presented by the soil, LABFIT software was employed for curve fitting using the generic formulation "Harris + C". The results of the tests indicated that the phenomenon of hysteresis had a greater influence in situations with higher suction levels. When comparing the residual moisture values of the macropores between residual soil and sedimentary soil, the former exhibited the lower value. This suggests that the residual soil has a coarser grain size and larger pores, which facilitates the release of water retained in the soil's macropores.

Key words: Soil-water characteristic curve, suction, filter paper method.

1. Introduction

To understand the behavior of processes in unsaturated soils, it is necessary to analyze the distribution, retention, and release of water under various conditions, whether mechanical or environmental. Phenomena such as infiltration, evaporation, and changes in external stress cause water to move into or out of the soil. Thus, by using a curve defined as a function of the variation in energy required to remove water (suction) and the retention capacity of water in the macropores and micropores within the soil, it is possible to analyze the soil's behavior in the presence of water [1-3]. The soil-water characteristic curve is defined as the graphical representation of the relationship between moisture (degree of saturation, volumetric or gravimetric moisture content) and suction (total, matric or osmotic suction) being the most important property for the mechanical analysis of unsaturated soils [1, 2, 4]. Therefore, this study aims to model the soil-water characteristic curve for soils collected at Bom Brinquedo Hill's, in Antonina, Brazil. This mountain range region is characterized as a natural disaster risk area, requiring continuous research related to the stability of the area.

1.1 Definition of the Study Area

The study area is located on the southern slope of Bom Brinquedo Hill's, in the county of Antonina, Paraná. Antonina is situated on the northern coast of the state of Paraná, in the Microrregion of Paranaguá, with predominantly mountainous relief, featuring plains to the center and south, along with several hills scattered throughout the municipality [5]. The study area is in a place called Buraco da Onça, on Bom Brinquedo Hill's, and is situated near the streets Thiago Peixoto, Isidoro Costa Pinto, 5 de Junho, and Nestor de Castro. The studied risk area covers approximately 80.000 m², with the water and sediment dispersion plain covering approximately 20.000 m². The area has been classified as having a very high risk of floods and inundations due

Corresponding author: Gislaine Klenk Malinoski, B.S., Civil Engineer, research fields: geotechnics and unsaturated soils.

to the large extent of the contributing basin, which can concentrate significant volumes of water during intense rainfall periods, and due to the proximity of urban occupation on the dispersion plain [6].

Regarding the geology of the study area, porphyritic granite predominates, characterized by a coarse and isotropic texture, with small areas of contribution from foliated amphibolite and foliated granite. The granite outcrops in large boulder fields (greater than 3 m in diameter), rock slabs, and vertical escarpments, primarily on the upper slopes and peaks of the relief [6].

In Bom Brinquedo Hill's, the transition from residual soil to transported soil along the slope occurs around the 60-m contour. The residual profile typically features a mature, clayey and compact soil layer, ranging in color from brown to dark yellow. This layer transitions gradually or diffusely into a layer of young, silty-sandy and compact soil, which is pinkish or light red in color and has a thickness similar to that of the mature soil. In the lower mid-slope and at the base of the slopes, sedimentary soil, or colluvial ramps, are present. These soils are typically unstable, as they are supported by a predominantly clayey matrix, with thickness increasing toward the base [6].

Table 1 presents a summary of the geological-geotechnical characterization of disturbed soil samples collected from the study area. Undisturbed samples from these five locations were also collected and will subsequently be subjected to suction testing and soil-water characteristic curve development.

2. Material and Methods

To determine the soil-water characteristic curve, suction testing was performed using the filter paper method, as standardized by ASTM D 5298 [7].

2.1 Materials

The materials required for the test were: Whatman filter paper No. 42, deaerated water, plastic film, aluminum foil, metal sampling cylinder, tweezers, scissors, latex gloves, plastic adhesive tape, self-sealing hermetic bags, hermetic Styrofoam box, drying chamber, oven, and analytical balance with a precision of 0.0001 g with weighing chamber.

2.2 Sampling

Sampling was carried out by collecting undisturbed samples from five distinct collection points in the study area. In the laboratory, ten samples were molded for each collection point in a circular metal ring with an approximate diameter of 4.8 cm and height of 2 cm. To determine the moisture-imposed interval, one sample from each collection point was saturated for approximately one day, allowing for the determination of a suction point near zero. Similarly, one sample from each collection point was dried to hygroscopic moisture to determine a point of suction close to the maximum. Once the upper and lower limits of moisture variation were determined, the ten samples from each collection point were divided into equal moisture intervals to ensure a good distribution of points with different suction levels, thus providing a more representative curve. The test was repeated three times for each sample, with two moisture measurement papers per sample, resulting in three hundred suction versus moisture pairs. The samples underwent moisture

Table 1 Geological-geotechnical characterization.

Collection point	Soil classification [6]	wn (%)	γ_n (kN/m³)	γ_d (kN/m³)	D	L_L (%)	L_P (%)	I_P (%)	e	n	Clay (%)	Silt (%)	Sand (%)	Gravel (%)
01	Granite residual	35.6	16.3	12.0	2.616	81	45	37	1.18	0.54	59.7	12.4	23.4	7.3
02	Granite residual	22.0	15.5	12.7	2.545	51	35	16	1.01	0.50	35.7	17.1	31.4	15.9
03	Colluvial Sedimentary	40.7	16.9	12.0	2.730	60	37	24	1.27	0.56	59.8	28.2	10.2	1.7
04	Granite residual	27.6	17.1	13.4	2.247	58	45	13	0.68	0.40	28.0	17.1	42.8	12.1
05	Colluvial Sedimentary	40.4	16.0	11.4	2.692	59	45	14	1.36	0.58	36.3	40.5	21.2	2.0

variation through drying and wetting processes, with results presented separately due to the phenomenon of hysteresis.

2.3 Suction Measurement

For the measurement of matric suction, two pieces of Whatman filter paper No. 42 were placed directly on the surface of the sample so that the papers encountered the pore water of the soil, with the flow being due only to capillary phenomena. The papers used were squares with 1 cm sides, ensuring that the total area of the paper was in contact with the soil surface to maximize the accuracy of moisture measurements. After establishing the desired moisture content in the sampled soil, the two papers were placed on the sample, having been weighed and dried in an oven beforehand. The sealing of the soil and filter paper sets was done by wrapping them in PVC (Polyvinyl Chloride) film, followed by aluminum foil, to prevent moisture loss or gain from the external environment, with two layers of each material intercalated. Finally, the set was protected with PVC plastic film to keep the paper firmly against the soil. The samples were stored in a hermetically sealed Styrofoam box and placed in a dry chamber (approximately 19 ℃) for 7 days to allow the system to equilibrate, followed by the subsequent measurement of the soil's matric suction. After the equilibrium period, the filter paper and the soil sample with the ring were weighed on a balance with a resolution of 0.0001 g to determine the wet paper mass. After determining the mass, the paper was placed in the oven for drying for 24 h (at approximately 105 ℃) to determine its dry mass. The soil samples were also weighed and measured after removing the paper to determine the dry density and to potentially correct the moisture values initially estimated at the beginning of the test.

2.4 Calibration Equation

After determining the equilibrium moisture content of the paper and the soil, Eq. (1) was used for calibration when the paper moisture (w_{paper}) content is less than or equal to 47%, and Eq. (2) was used for paper moisture contents greater than 47% [8]:

$$10^{4.84-0.0622\ w_{paper}(\%)} \quad (1)$$

$$10^{6.05-2.48\ log\ [w_{paper}(\%)]} \quad (2)$$

2.5 Curve Fitting Equation

Upon obtaining the volumetric moisture versus suction curve, the data were fitted to empirical relationships commonly used in the literature, such as those by Van Genuchten [9] and Fredlund et al. [10]. However, a satisfactory fit could not be achieved, as these mathematical relationships are designed for unimodal curves, whereas the soil exhibited a bimodal characteristic. Therefore, the LABFIT software [11] was used for curve fitting through non-linear regression applied iteratively until a convergence criterion for the data collection points was reached. To this end, equations were sought that provided a better fit to the different levels formed by the experimental points, ensuring an adequate representation of the soil-water characteristic curve for each sample. Similarly to Ferreira [12], the equations were adjusted using the generic formulation known as "Harris + C", as shown in Eq. (3):

$$Y = \frac{1}{(A + B * X^C)} + D \quad (3)$$

where *A*, *B*, *C* and *D* represent the curve fitting parameters; *Y* is the estimated suction (kPa); and *X* is the volumetric water content (m^3/m^3).

3. Results and Discussion

The soil-water characteristic curve was defined by two equations, for drying and wetting, with each interval being delimited by the suction levels presented for each sample. The soil-water characteristic curve can be divided into three segments, each corresponding to a different parameter. The first segment corresponds to the saturated zone, which ends at the suction value where air enters, directly related to the maximum suction that the larger pores of the soil can withstand without drainage occurring. The second suction

interval corresponds to the desaturation zone, where water is drained in terms of liquid flow, as it is in a relatively free condition within the soil pores. Finally, the degree of saturation in the residual zone corresponds to the exit of water, which is relatively less free than in the previous segment and occurs predominantly through vapor transfer processes, associated with high suction values [3].

The soil-water characteristic curve was represented for the wetting and drying processes separately, highlighting the hysteresis phenomenon. Thus, the curves that fit the experimental data for residual soils are shown in Fig. 1, and for colluvial sedimentary soils in Fig. 2.

3.1 Soil-Water Characteristic Curves for Residual Soil

Collection points 01, 02, and 04 were classified as residual soils and exhibited an average porosity of 49.3%. The results from the three collection points showed some dispersion between them, particularly for suction data between 0 and 10 kPa. The wetting curve that fits all the data for the residual soil was represented by Eq. (4) for the suction range of 0 to 5 kPa, and by Eq. (5) for suction values above 5 kPa.

$$\theta_{w1,r} = \frac{1.00}{(5.00 + 10^{-3} * \psi^{5.00})} + 0.29 \quad (4)$$

$$\theta_{w2,r} = \frac{1.00}{(2.23 + 0.03 * \psi^{0.49})} - 0.10 \quad (5)$$

where $\theta_{w1,r}$ is the suction for the first part of the wetting curve of the residual soil (kPa), $\theta_{w2,r}$ is the suction for the second part of the wetting curve of the residual soil (kPa), and ψ is the volumetric water content (m^3/m^3).

For the fitting of the drying curve corresponding to the residual soil data, Eq. (6) was used for suction values between 0 and 10 kPa. For values greater than 10 kPa, Eq. (7) provided a better fit to the experimental data for the residual soil.

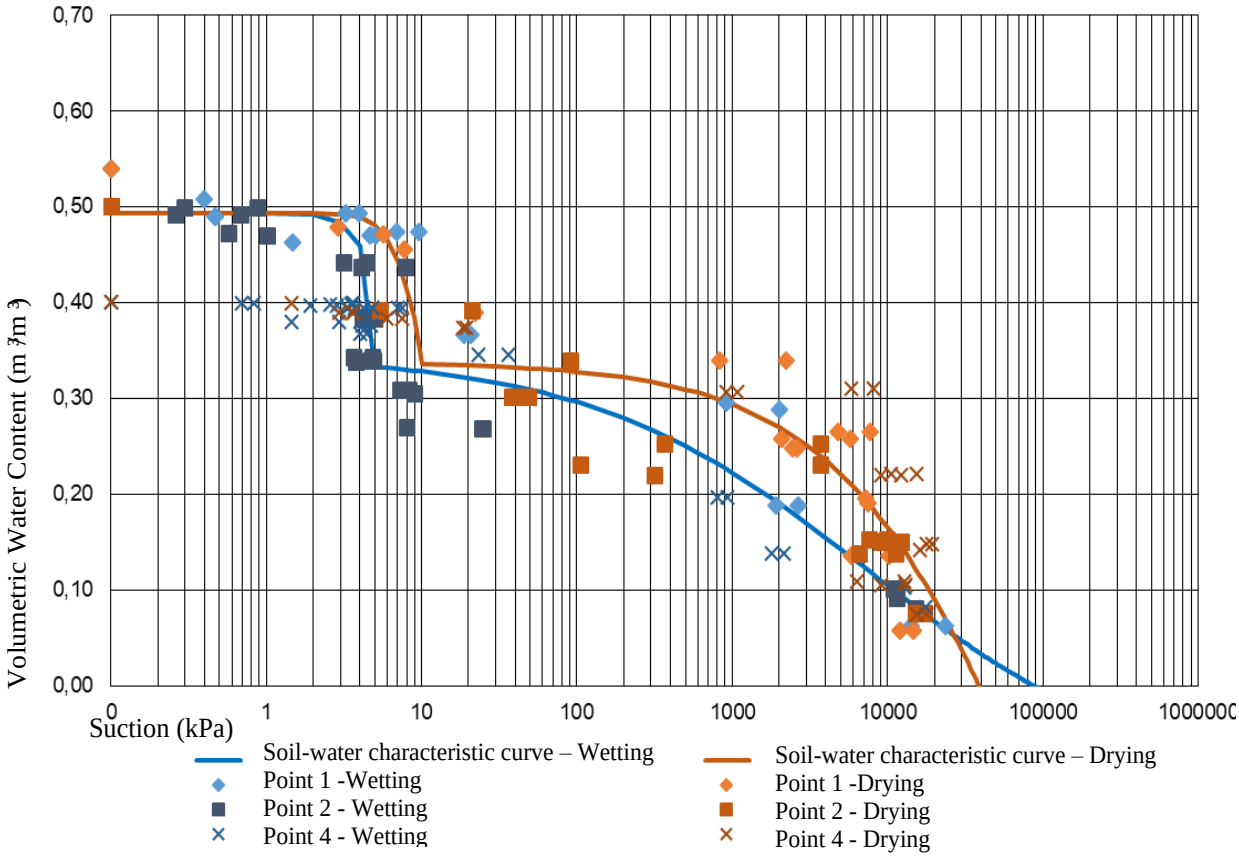

Fig. 1 Soil-water characteristic curves for residual soil.

$$\theta_{d1,r} = \frac{1.00}{(5.00 + 10^{-4} * \psi^{5.00})} + 0.29 \quad (6)$$

$$\theta_{d2,r} = \frac{1.00}{(0.97 + 4.72 * 10^{-4} * \psi^{0.65})} - 0.69 \quad (7)$$

where $\theta_{d1,r}$ is the suction for the first part of the drying curve of the residual soil (kPa), $\theta_{d2,r}$ is the suction for the second part of the drying curve of the residual soil (kPa), and ψ is the volumetric water content (m^3/m^3).

Up to a suction of 5 kPa, the drying and wetting curves exhibited similar behavior. Among the three residual soil collection points tested, the results from collection point 04 showed greater dispersion compared to the other two, which can be explained by the coarser particle size composition of this collection point, with 42.8% sand.

The equations provided a good fit to the data, with air entry pressures in the macropores of 3.3 and 5.5 kPa for the wetting and drying curves, respectively. The residual moisture content in the macropores for both curves was approximately 32%. The hysteresis phenomenon was more pronounced in the case of higher suctions. Therefore, the air entry pressure in the micropores was observed to be approximately 100 kPa for the wetting curve and 800 kPa for the drying curve.

3.2 Soil-Water Characteristic Curves for Sedimentary Soil

The results from collection points 03 and 05 were plotted together to obtain the soil-water characteristic curve for colluvial sedimentary soil. The two segments presented by the wetting and drying curves varied between 0 and 10 kPa, and for values greater than 10 kPa. Therefore, Eq. (8) represents the wetting curve for suction values between 0 and 10 kPa, and Eq. (9) for values above 10 kPa.

$$\theta_{w1,c} = \frac{1.00}{(10.13 + 7.94 * 10^{-4} * \psi^{4.82})} + 0.46 \quad (8)$$

$$\theta_{w2,c} = \frac{1.00}{(2.27 + 1.94 * 10^{-8} * \psi^{2.11})} + 0.01 \quad (9)$$

where $\theta_{w1,c}$ is the suction for the first part of the wetting curve of the colluvial soil (kPa), $\theta_{w2,c}$ is the suction for the second part of the wetting curve of the colluvial soil (kPa), and ψ is the volumetric water content (m^3/m^3).

The suction values for the colluvial soil showed little dispersion between the two collection points, resulting in equations with excellent fit to the experimental data. The experimental points for the drying curve were fitted using Eq. (10) for suction values between 0 and 10 kPa, while Eq. (11) represents the soil-water characteristic curve for suction values above 10 kPa. The following are the representative equations for the drying curve of the colluvial soil, based on the sampled collection points.

$$\theta_{d1,c} = \frac{1.00}{(8.74 + 0.01 * \psi^{3.25})} + 0.45 \quad (10)$$

$$\theta_{d2,c} = \frac{1.00}{(2.23 + 1.39 * 10^{-9} * \psi^{2.29})} + 4.24 * 10^{-4} \quad (11)$$

where $\theta_{d1,c}$ is the suction for the first part of the drying curve of the colluvial soil (kPa), $\theta_{d2,c}$ is the suction for the second part of the drying curve of the colluvial soil (kPa), and ψ is the volumetric water content (m^3/m^3).

The residual moisture content of the macropores for the colluvial soil was the same for both the drying and wetting curves, defined as 42.5%. The air entry pressure for the micropores for the wetting curve was 2.200 kPa, while for the drying curve, it was 3.500 kPa. Thus, the hysteresis phenomenon occurred for suction values above 1.000 kPa, showing lower values for the same moisture content when compared to the residual soil. Finally, the residual moisture content of the micropores was approximately zero for both the drying and wetting curves.

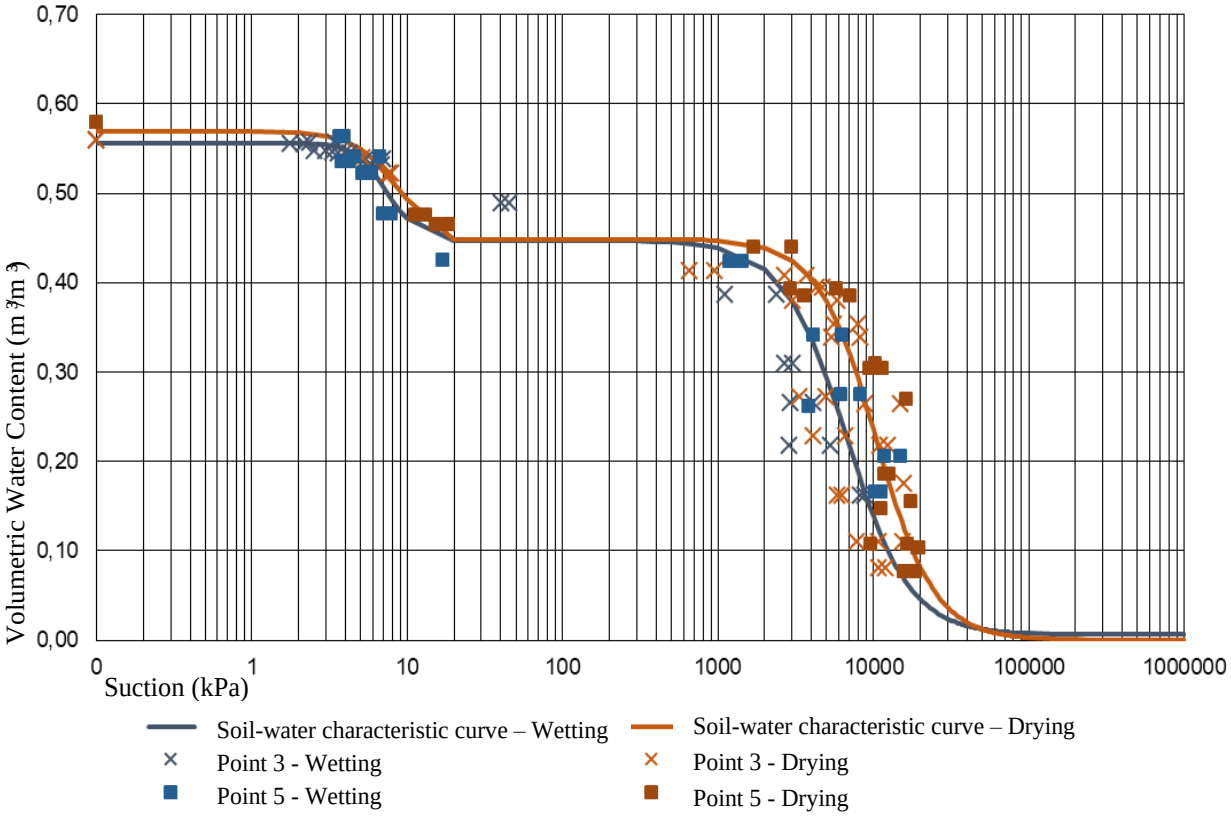

Fig. 2 Soil-water characteristic curves for sedimentary soil.

4. Conclusions

The soil-water characteristic curve allows for the determination of residual moisture contents and air entry pressures for each type of pore. All the soils studied exhibited a bimodal shape, indicating the presence of macropores and micropores. Therefore, it was not possible to fit the data to the empirical relationships commonly used in the literature, such as those of Van Genuchten [9] and Fredlund et al. [10], as these mathematical relationships are designed for unimodal curves.

The suction test results indicated that the hysteresis phenomenon had a greater influence in situations where higher suction levels were present. Additionally, the sandy soil tested showed more pronounced hysteresis compared to the other samples, which had finer granulometry. Regarding the suction test, of the three residual soil collection points tested, the results from collection point 04 showed the greatest dispersion when compared to the other two, which can be explained by the coarser granulometric composition of this collection point, which contains 42.8% sand. On the other hand, the suction values for the colluvial soil showed little dispersion between the two collection points, resulting in equations that provided a good fit to the experimental data. When comparing the residual moisture content of the macropores between the residual soil (32%) and the colluvial soil (42.5%), the former showed the lower value. In other words, the residual soil has a coarser granulometry and larger pores, which facilitates the release of water retained in the macropores of the soil.

Acknowledgments

The authors would like to thank the PPGEC (Post-Graduation Program in Civil Engineering), the UFPR (Federal University of Paran â), for making the possible accomplishment of this research project.

References

[1] Fredlund, D. G. 2002. "Use of the Soil-Water Characteristic Curve in the Implementation of Unsaturated Soil Mechanics." In *Proceedings of the Third International Conference on Unsaturated Soils, UNSAT 2002*, Recife, Brazil, pp. 887-902.

[2] Soto, M. A. A. 2004. "Comparação entre métodos de imposição e de controle de sucção em ensaios com solos não saturados." Ph.D. thesis, Universidade de São Paulo. (in Portuguese)

[3] Gitirana Jr., G. F. N., Marinho, F. A. M., and Soto, M. A. A. 2015. "A curva de retenção de água de materiais porosos." In *Solos não saturados no contexto geotécnico* (Cap. 9), edited by J. C. CARVALHO, et al. São Paulo: Associação Brasileira de Mecânica dos Solos e Engenharia Geotécnica, pp. 205-29. (in Portuguese)

[4] Fredlund, D. G. 2006. "Unsaturated Soil Mechanics in Engineering Practice." *Journal of Geotechnical and Geoenvironmental Engineering* 132 (3): 286-321.

[5] Prefeitura Municipal de Antonina. 2019. "História. Paraná, Brasil." Accessed 2 July 2019. http://antonina.pr.gov.br/pagina/78_Historia.html. (in Portuguese)

[6] Mineropar. 2013. *Minerais do Paraná S.A. Avaliação geotécnica de vertentes na área urbana de Antonina.* Curitiba: Mapas. (in Portuguese)

[7] ASTM (American Society for Testing Materials). 2003. *5298-03: Standard Test Method for Measurement of Soil Potential (Suction) Using Filter Paper*. Pennsylvania: West Conshohocken.

[8] Marinho, F. A. M., Soto, M. A. A., and Gitirana Jr., G. de F. N. 2015. "Instrumentação de laboratório e campo e a medição da curva de retenção." In *Solos não saturados no contexto geotécnico* (Cap. 10), edited by J. C. Carvalho et al. São Paulo: Associação Brasileira de Mecânica dos Solos e Engenharia Geotécnica, pp. 231-56. (in Portuguese)

[9] Van Genuchten, M. T. 1980. "A Closed-Form Equation for Predicting the Hydraulic Conductivity of Unsaturated Soils." *Soil science society of America Journal* 44 (5): 892-8.

[10] Fredlund, D. G., Xing, A., and Huang, S. 1994. "Predicting the Permeability Functions for Unsaturated Soil Using the Soil Water Characteristics Curve." *Canadian Geotechnical Journal* 31 (4): 533-46.

[11] Silva, W. P., e Silva, C. M. D. P. S., Cavalcanti, C. G. B., e Silva, D. D. P. S., Soares, I. B., Oliveira, J. A. S., and e Silva, C. D. P. S. 2004. "LAB Fit Ajuste de Curvas: Um software em português para tratamento de dados experimentais." *Revista Brasileira de Ensino de Física* 26 (4): 419-27. (in Portuguese)

[12] Ferreira, K. S. D. M. 2017. "Análise hidromecânica de um talude rodoviário composto por solo residual no trecho de Serra do Mar da BR-376/PR." Trabalho de Conclusão de Curso (Graduação em Engenharia Civil), Universidade Federal Do Paraná, Curitiba. (in Portuguese)